

An Analytical Method of Micropore Filling of a Supercritical Gas

K. KANEKO AND K. MURATA

Department of Chemistry, Faculty of Science, Chiba University, 1-33 Yayoi, Inage, Chiba 263, Japan

Received April 5, 1996; Revised August 20, 1996; Accepted September 10, 1996

Abstract. The supercritical gas adsorbed in the micropore having a strong molecular field was presumed to transform into the quasi-vapor to be filled in the micropore (quasi-vaporization adsorption mechanism). The Dubinin-Radushkevich (DR) equation for micropore filling of vapor was extended to the quasi-vaporized supercritical gas using the quasi-saturated vapor pressure P_{0q} and the inherent micropore volume W_L . The reason why the concepts of P_{0q} and W_L were introduced was explained with the molecule-pore interaction potential theory which is based on the Lennard-Jones interaction. The extended DR equation was named the supercritical DR equation. The W_L was evaluated by the Langmuir plot of the adsorption isotherm for a supercritical gas and both of P_{0q} and W_L provided the single reduced adsorption isotherm which can describe the adsorption isotherms of different samples at different temperatures. The adsorption isotherms of supercritical NO, N₂, and CH₄ on activated carbon fibers and high surface area carbons were analyzed by the supercritical DR plots. The wide applicability of the reduced adsorption isotherm to these adsorption data was explicitly shown. The two phase model of the organized and confined fluids was proposed in order to improve the quasi-vaporization adsorption mechanism.

Keywords: micropore filling, supercritical gas, carbon micropore, nitrogen monoxide, methane, molecular assembly

1. Introduction

There are many important gases of supercritical gases whose critical temperature is lower than an ambient temperature. O₂, N₂, NO, CO₂, CO, H₂, and CH₄ are representatives of a supercritical gas near room temperature. The adsorption of these supercritical gases has been deeply associated with gas separation, gas storage, catalysis, supercritical extraction, supercritical drying, and pollution control. Thus, these gases are essentially important from the practical and fundamental aspects. The progress in the adsorption science for a supercritical gas has been expected from the advanced technology. The supercritical gas which has no concept of the saturated vapor pressure cannot be adsorbed on the flat surface, macropores, and even mesopores with physical adsorption.

The adsorption of vapor by micropores, which is called micropore filling, is enhanced at a very low pressure region due to overlapping of the molecule [·]

pore-wall interactions. The deep potential well of the micropore gives rise to even adsorption of the supercritical gas to some extent. Still the micropore cannot adsorb abundant amount of the supercritical gas. That is, the quite narrow micropore whose width is fit for the size of the adsorbate molecule has a very deep molecular potential well and is effective even for adsorption of the supercritical gas. However, the amount of adsorption by such a narrow micropore is limited to much less than the micropore volume, because the potential barrier for the intrapore diffusion is greater than thermal energy in the narrow micropore. For example, if the graphitic slit-micropore consists of narrow and wide parts of 0.48 and 0.56 nm in width, the N₂-graphitic micropore potential difference per k_B is about 400 K, which works as the potential barrier for the diffusion; the strongly adsorbed molecule of the supercritical gas near the micropore entrance blocks the further adsorption. Accordingly, the supercritical gas is not an objective gas for a predominant micropore

filling. In case of micropore filling of vapor, the potential well of the micropore whose width is even more than trilayer thickness of the molecular size is enough deep that the vapor molecules can be sufficiently filled at a low pressure region without any obstacle for the intrapore diffusion.

Adamson mentioned "Physical adsorption is usually important only for gases below their critical temperature, that is, for vapors", in his famous book (Adamson, 1990). The supercritical gas has no coexistent conditions with liquid, while vapor coexists with liquid. Hence vapor tends to form a liquid like film on the solid surface, inducing a predominant physical adsorption in principle, although it depends on the difference between the molecule-surface interaction and the intermolecular interaction. Then the established theory of physical adsorption has used the saturated vapor pressure P_0 as the standard. P_0 is indispensable to describe usual physical adsorption processes. On the other hand, P_0 cannot be defined for a gas above the critical temperature T_C . Consequently, almost analytical methods for physical adsorption such as BET and Dubinin-Radushkevich (DR) plots cannot be applied to the adsorption of a supercritical gas. Further, no profound adsorption of a supercritical gas even by a microporous system has been realized under the subatmospheric pressure of the adsorptive gas. The application of the high pressure above the ambient pressure (high pressure experiment) is necessary for balancing the high chemical potential of the adsorbate in the micropore. The analytical method for physical adsorption of a supercritical gas is much less advanced compared with physical adsorption of vapor (Gregg and Sing, 1982; Jaroniec and Madey, 1988; Rudzinski and Everett, 1992), although many empirical equations have been used for description of physical adsorption of a supercritical gas (Wakasugi, Ozawa and Ogino, 1981). The DR analysis has contributed to describe the micropore filling of various vapors (Dubinin, 1960, 1987), although what the Henry law cannot be derived from the DR equation at a low pressure limit has been criticized. As recently it was shown that both of DR and Henry equations can be derived from the identical model equation (Cheng and Yang, 1995), the general applicability was assured more. The extension of the DR analysis to a supercritical gas is preferable for comparison of the knowledge on the micropore filling for vapor.

Molecular simulation studies are based on the Lennard-Jones (LJ) interaction and the LJ parameters

are used for both vapor and supercritical gases (Balbuena and Gubbins, 1992; Bojan et al., 1996; Cracknell et al., 1995; Dunne et al., 1996). Accordingly the molecular simulation approach can describe the adsorption process of a supercritical gas by a micropore and we can compare the observed adsorption isotherm with the simulated one even for a supercritical gas. However, we also need a simple analytical method for getting physical insights from experimental data.

Kaneko prepared a remarkable microporous adsorbent for a supercritical NO under a subatmospheric pressure about 9 years ago (Kaneko, 1987, 1988, 1989). It was noteworthy that iron oxide-dispersed activated carbon fibers (Fe-ACF) can adsorb a great amount of NO of more than 300 mgg^{-1} in the micropores at 303 K and 80 kPa. Supercritical NO can be as rapidly and sufficiently adsorbed on Fe-ACF like an organic vapor on them. The noticeable micropore filling of supercritical NO on Fe-ACF is caused by the transformation of the supercritical gas to vapor through dimerization (Kaneko et al., 1987, 1988). Such dimerization occurs in other supercritical gases more or less. The simple description of adsorption of a supercritical gas by a microporous solid is indispensable to understand and control the micropore filling of a supercritical gas.

Activated carbon fibers (ACFs) and superhigh surface area carbons (HSAC) have considerably uniform micropores compared with conventional activated carbons (Kakei et al., 1991; Kaneko and Ishii, 1992; Kaneko et al., 1992; Rao et al., 1992; Setoyama et al., 1992). The adsorption experiments of supercritical gases on ACFs or HSAC should provide reliable data for construction of a new analytical method for micropore filling of a supercritical gas.

In this article, the extension of the DR analysis to the micropore filling of a supercritical gas is introduced and the availability is shown for supercritical NO, N_2 , and CH_4 .

2. Difference between Vapor and Supercritical Gas

The state of matter is described in terms of the pressure P , the molar volume V_m , and the temperature T (Atkins, 1990). Then three phases of gas, liquid, and solid are expressed by the P - V_m - T profile, as shown

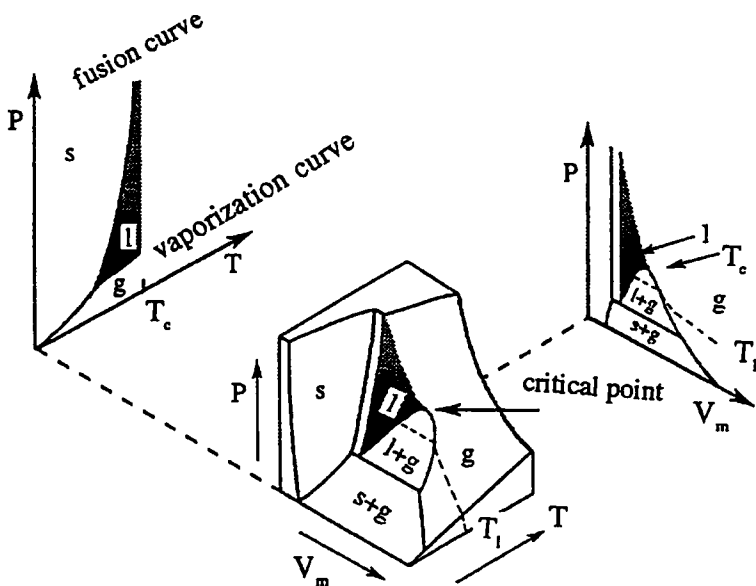


Figure 1. The phase diagram of matter.

in Fig. 1. Figure 1 also shows the $P-T$ and $P-V_m$ projections. The $P-V_m$ projection indicates the presence of the coexistent region of gas and liquid in equilibrium, which is designated by $(l+g)$. The broken line parallel to the abscissa of the $P-V_m$ projection at a temperature T_l denotes the coexistent region. The section of the isotherm becomes less and less, as the temperature is raised. Finally the isotherm is reduced to a mere point whose temperature is called the critical temperature. The critical temperature T_c is the maximum temperature at which a gas can be liquefied and above T_c liquid cannot coexist. The pressure for liquefaction at T_c is called the critical pressure. We can see the vaporization curve between liquid and gas on the $P-T$ projection. Above T_c there is no vaporization curve and no distinction between liquid and gas. Therefore, we must distinguish the gaseous states above and below T_c . The term vapor is used to describe a gaseous substance when its temperature is below T_c and the vapor can be condensed to a liquid by pressure alone. However, the gas above T_c , which is called a supercritical gas, cannot be liquefied even at quite high pressures.

Thus, vapor has own saturated vapor pressure P_0 . Then we can use the relative pressure P/P_0 only for description of adsorption of vapor. On the other hand, the supercritical gas has no concept of the saturated vapor pressure. The relative pressure expression cannot be used for description of adsorption of a supercritical gas.

3. Deep Potential Well for Adsorption of Supercritical Gas

The interaction between an admolecule and a surface atom as a function $\Phi(r)$ of the distance r between them can be expressed by the Lennard-Jones potential,

$$\Phi(r) = 4\epsilon_{sf}[(\sigma_{sf}/r)^{12} - (\sigma_{sf}/r)^6] \quad (1)$$

where ϵ_{sf} and σ_{sf} are the potential well depth and effective diameter for the admolecule-graphitic carbon atom. These cross parameters are calculated according to the Lorentz-Berthelot rules, $\epsilon_{sf} = (\epsilon_{ss}\epsilon_{ff})^{1/2}$; $\sigma_{sf} = (\sigma_{ss} + \sigma_{ff})/2$. Here, $(\sigma_{ss}, \epsilon_{ss})$ and $(\sigma_{ff}, \epsilon_{ff})$ are the Lennard-Jones parameters for a surface atom and a fluid molecule, respectively. The interaction potential $\Phi(z)$ for an admolecule and a single graphite slab is given by the Steele 10-4-3 potential (Steele, 1973),

$$\Phi(z) = 2\pi\rho_C\epsilon_{sf}\sigma_{sf}^2\Delta\{(2/5)(\sigma_{sf}/\delta)^{10} - (\sigma_{sf}/\delta)^4 - \sigma_{sf}^4/[3\Delta(0.61\Delta + \delta)^3]\} \quad (2)$$

where δ is the vertical distance of the admolecule above the surface, Δ is the separation between graphite layers ($= 0.335$ nm), ρ_C is the number of carbon atoms in a graphite layer ($= 114$ nm $^{-3}$). The exponent-10 and 4 terms denote the repulsive and attractive interactions

of the molecule with the surface graphite plane, while the exponent-3 term results from the summation of the attractive part of the potential over the subsurface layers of the graphite. As the micropores of activated carbon can be approximated by the slit spaces between the predominant basal planes of micrographitic units, the whole interaction potential $\Phi(z)_p$ of a molecule with the micropore of an inter-graphite surface distance H can be given by Eq. (3).

$$\Phi(z)_p = \Phi(z) + \Phi(H - z) \quad (3)$$

Consequently, we can evaluate the potential profile of the molecule adsorbed in the graphitic micropore. Here H is not the effective pore width w determined by the adsorption experiment. The relationship between H and w is expressed by Eq. (4) (Kaneko et al., 1994).

$$H = w + 0.8506\sigma_{sf} - \sigma_{ff} \quad (4)$$

In the case of the N_2 -graphitic slit pore system, w is equal to $H - 0.24$ nm. Figure 2 shows potential profiles of N_2 and CH_4 in a slit-shaped graphite pore as a function of w using the one-center approximation. Here, the molecular position in Fig. 2 is expressed by a distance z from the central plane between two surfaces. The broken line shows the potential profile for the single graphite surface. The potential becomes deeper with decrease in the w value. The potential profile has double minima for $w > 0.6$ nm, but a narrower pore has a single potential minimum. Thus, micropores have stronger adsorption fields than flat or mesoporous surfaces. The depth of the potential well for vapor is enough great to lead to the Type I adsorption isotherm, i.e., an enhanced adsorption at a low relative pressure range, being characteristics of micropore filling.

Activated carbon has abundant micropores and their adsorption field can be approximated by the above mentioned graphite-slit space model. As the interaction potential at the mid-point of the slit-pore is the deepest in the pore of $w < 0.6$ nm and it is not seriously different from the double minima even for $w > 0.6$ nm, the molecular potential for a molecule in the micropore can be approximated by the potential at the mid-point of the slit-pore. If we use the more simple 9-3 potential than the 10-4-3 potential, the potential energy minimum $\Phi(H/2)_p$ at the midpoint

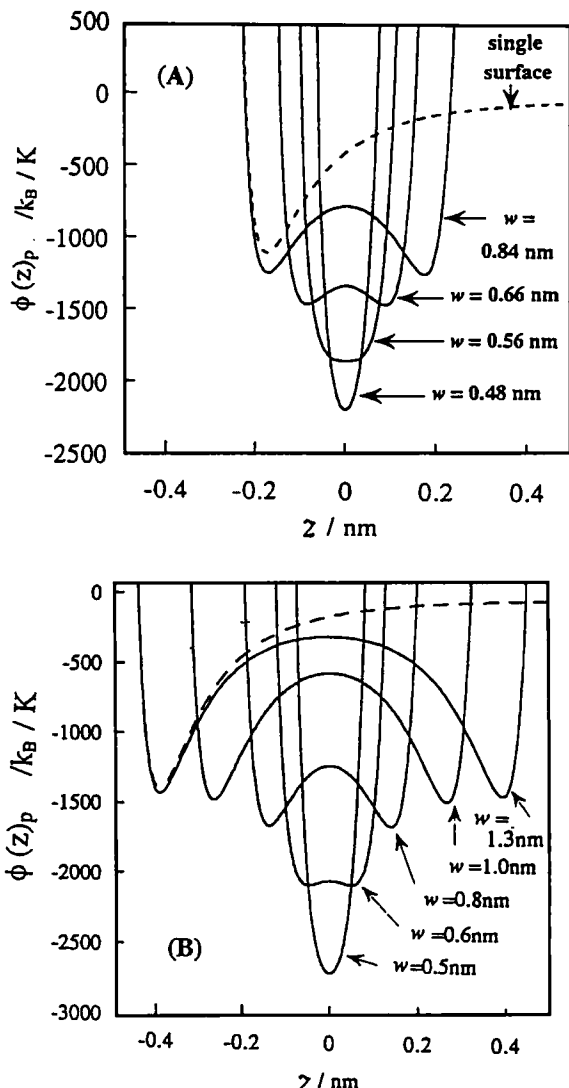


Figure 2. Potential profile of N_2 (A) and CH_4 (B) with the graphitic slit-pore as a function of pore width w .

(at $z = H/2$) between the two surfaces is approximated by Eq. (5).

$$\Phi(H/2)_p = 2\Phi(H/2) \quad (5)$$

Here ε_{gr} is the interaction energy minimum of a molecule with a single graphite surface and $2d$ ($= H$) is the internuclear distance of two parallel graphite surfaces. When d is approximated by $w + 2r_C$ (radius of a carbon atom), $\Phi_{gr}(0)$ is given by Eq. 6. Thus, the average potential depth is simply expressed

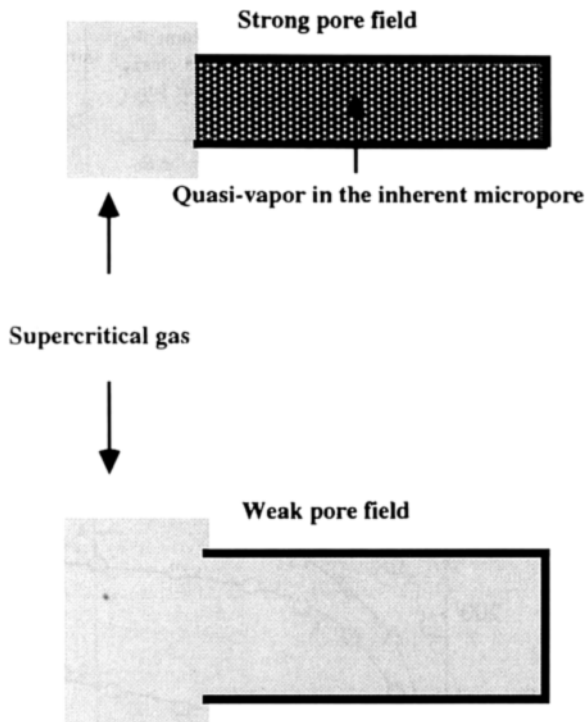


Figure 3. The model of the micropore space which induces transformation of a supercritical gas to the vapor.

by the pore width w . If the adsorption potential $A [= RT \ln(P_0/P)]$ of an adsorbed molecule is associated with the molecular potential energy after Hill's approach (Hill, 1952; Horvath and Kawazoe, 1983) and the molecules are adsorbed in the micropore having the strong potential of $\Phi(H/2)_p$, according to the Boltzmann distribution, the next intrapore-field dependent micropore filling (IFMF) equation is obtained.

$$RT \ln(W_L/W) = \Phi(H/2)_p + U^{\text{CO}} \quad (6)$$

Here W_0 is the micropore volume determined from N_2 adsorption at 77 K, W_L is the micropore volume which has enough strong adsorption field to adsorb a supercritical gas at adsorption temperature and N_A is the Avogadro's number. We designate the W_L inherent micropore volume for each supercritical gas, which is governed by the micropore field. U^{CO} is the additional potential energy due to molecules already adsorbed (Kaneko et al., 1992).

The molecular potential theory supports the presence of W_L for each adsorptive, which depends on the

pore width w and characteristic quantities of ε_{gr} and σ_{sf} . This W_L can be determined experimentally due to a considerably strong adsorption which provides the Langmuir type isotherm. The W_L for vapor molecules is almost equal to the micropore volume W_0 obtained from N_2 adsorption at 77 K; the Gurvitch rule is held. On the other hand, W_L for a supercritical gas, which can be evaluated from the Langmuir plot of the adsorption isotherm, is less than W_0 .

4. The Modified DR Equation for a Supercritical Gas

The following DR equation can describe the micropore filling of vapor very well (Bering et al., 1966).

$$W/W_0 = \exp[-(A/E)^2], \quad E = \beta E_0 \quad (7)$$

Here W is the amount of adsorption at P , E_0 the characteristic adsorption energy, and β the affinity coefficient. βE_0 is associated with the isosteric heat of adsorption, $q_{\text{st},\phi=1/e}$, at the fractional filling ϕ of $1/e$ using the enthalpy of vaporization, ΔH_v , at the boiling point.

$$q_{\text{st},\phi=1/e} = \Delta H_v + \beta E_0 \quad (8)$$

As the saturated vapor pressure P_0 is not defined for a supercritical gas, the DR equation is not valid for description of adsorption of a supercritical gas. Although Dubinin estimated the saturated vapor pressure of the supercritical gas as an adsorptive by extrapolation of the pressure vs. temperature relationship (Dubinin, 1960) and tried to apply the DR equation to adsorption of a supercritical gas by microporous carbons, the approach has no physical basis on the concept of the saturated vapor pressure for the adsorptive of the supercritical gas. We need a concise analytical method for a supercritical gas from the experimental view point (Jagiello et al., 1995; Drago et al., 1996) in addition to the molecular statistical calculation.

It is presumed that supercritical gaseous molecules are concentrated in the micropore space by the strong molecule-pore interaction to induce an enhanced intermolecular interaction and the supercritical gas is transformed into a quasivapor. The quasi-vapor states depend strongly on the micropore width as mentioned above and the quasi-vapor should have own intermolecular structure (Kaneko, 1996) and the quasi-saturated vapor pressure P_{0q} . Each quasi-vapor has its inherent

micropore volume W_L and it can be filled in the micropore of the capacity W_L with the micropore filling mechanism. Hence, the DR equation can be extended to the quasi-vapor of the supercritical gas, as follows (Kaneko, 1989):

$$[\ln(W_L/W)]^{1/2} = (RT/\beta E_0)(\ln P_{0q} - \ln P) \quad (9)$$

The plot of $[\ln(W_L/W)]^{1/2}$ vs. $\ln P$ leads to both values of P_{0q} of the supercritical gas in the quasi-vapor state under the micropore field and βE_0 , that is, $q_{st,\phi=1/e}$. This plot is called the supercritical DR plot. The supercritical DR plot is quite useful to obtain the important information on adsorption of a supercritical gas through P_{0q} and $q_{st,\phi=1/e}$.

This supercritical DR equation gives the reduced adsorption isotherm of the supercritical gas using the concepts of P_{0q} and W_L which is experimentally estimated by the Langmuir plot of the adsorption isotherm. P_{0q} and W_L are related to the intermolecular interaction of supercritical gas in the quasi-vaporized state and the molecule-pore interaction, respectively. If the amount of adsorption W at a pressure P and the pressure are expressed by the fractional filling of W/W_L and the quasi-relative pressure P/P_{0q} , the reduced adsorption isotherm is obtained. It is given by the reduced DR equation of Eq. (8).

$$W = W_L \exp[-\{(RT/\beta E_0) \ln(P_{0q}/P)\}^2] \quad (10)$$

5. Micropore Filling of Supercritical NO

Supercritical NO is a representative component of acidic precipitations. An efficient adsorption of supercritical NO by microporous solids has been desired in order to concentrate the diluted NO emissions from automobiles for the perfect removal. However, there was no good adsorbent for supercritical NO before development of the iron oxide-dispersed activated carbon fiber (Fe-ACF). The adsorption isotherms of NO on Fe-ACF at different temperatures are shown in Fig. 4. These are Langmurian. Although all adsorption isotherms have a remarkable hysteresis, only the desorption branch at 274 K is shown. This hysteresis is not ascribed to chemisorption, but mainly to the dimerization of NO molecules. The amount of NO adsorption decreases with the increase of the adsorption temperature. Fe-ACF can adsorb abundant NO molecules at 303 K even below 101 kPa of NO (Kaneko, 1987, 1988; Wang

Table 1. Inherent micropore volume W_L , saturated vapor pressure P_{0q} , and characteristic adsorption energy βE_0 for supercritical NO on Fe-ACF.

Temperature K	W_L mlg^{-1}	P_{0q} kPa	βE_0 kJmol^{-1}
274	0.32	360	10.0
303	0.23	230	11.5
373	0.17	370	12.4

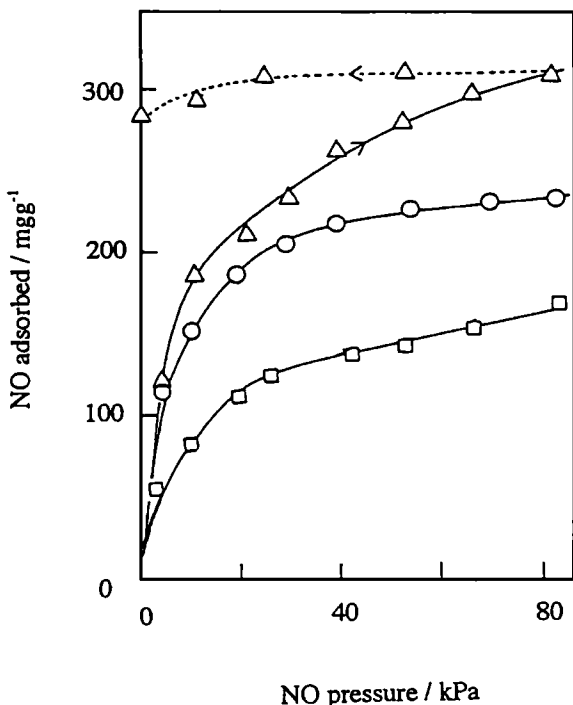


Figure 4. The adsorption isotherms of NO on Fe-ACF at different temperatures. Δ : 274 K, \circ : 303 K, \square : 373 K.

et al., 1992). The saturated amount of NO adsorption, $W_L(\text{NO})$, determined by the Langmuir plot provides the supercritical DR plot, as shown in Fig. 5. All supercritical DR plots are linear, supporting the quasi-vaporization adsorption mechanism of supercritical NO. We evaluated both of P_{0q} and βE_0 at each temperature, as shown in Table 1. Here, the inherent micropore volume $W_L(\text{NO})$ in mlg^{-1} is also listed using the liquid density of NO (1.06 gml^{-1}). The P_{0q} values are greater than 101 kPa, but they are in a reasonable range. On the contrary the estimated value of the saturated vapor pressure with the Dubinin's method (Dubinin,

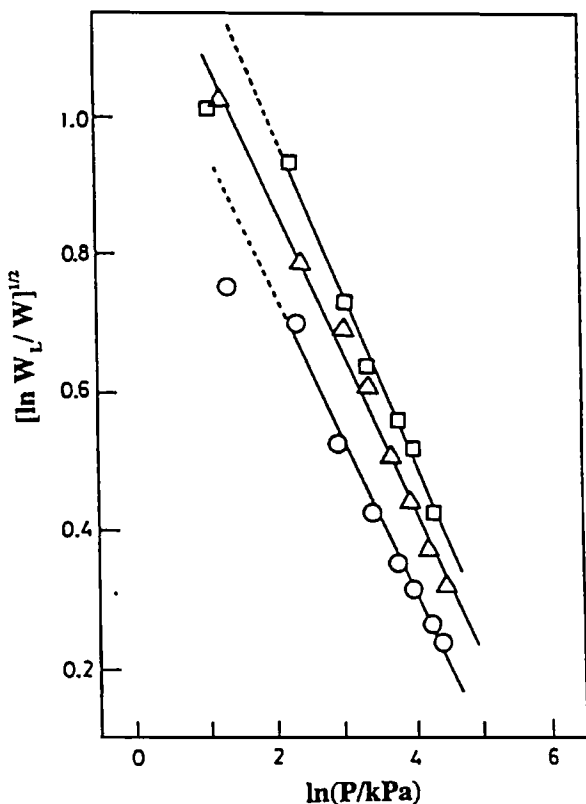


Figure 5. The supercritical DR plots of NO adsorption isotherms of Fe-ACF. Δ : 274 K, \circ : 303 K, \square : 373 K.

1960) goes over 1 GPa. The $q_{st,\phi=1/e}$ for NO is easily derived from Eq. (6) using ΔH_v of 13.8 kJmol^{-1} . The previous magnetic susceptibility measurement showed that the stabilization energy of the NO dimer in the micropore of ACF is 22–24 kJmol^{-1} , which is close to the $q_{st,\phi=1/e}$ for NO (Kaneko et al., 1989). Accordingly, the supercritical DR analysis is a hopeful and concise analytical method for adsorption of a supercritical gas.

The W_L and P_{0q} values give the reduced adsorption isotherm, as shown in Fig. 6. Three different adsorption isotherms in Fig. 4 are well expressed by a single reduced adsorption isotherm irrespective of the different adsorption temperature. The goodness of the reduced adsorption isotherm also supports a powerful applicability of the supercritical DR method proposed above.

Recently supercritical NO forms the clathrate compound with H_2O in the graphitic micropore without any application of the high pressure (Fujie et al., 1995). As H_2O adsorbed in the micropore has an ordered structure by *in situ* X-ray diffraction, NO molecules are incorporated in the void space of the H_2O network structure (Iiyama et al., 1995), this clathrate formation should stem from the presence of the very deep potential well of the organized water network. Thus, there is a possibility that the addition of other molecules can change the supercritical nature of a supercritical gas.

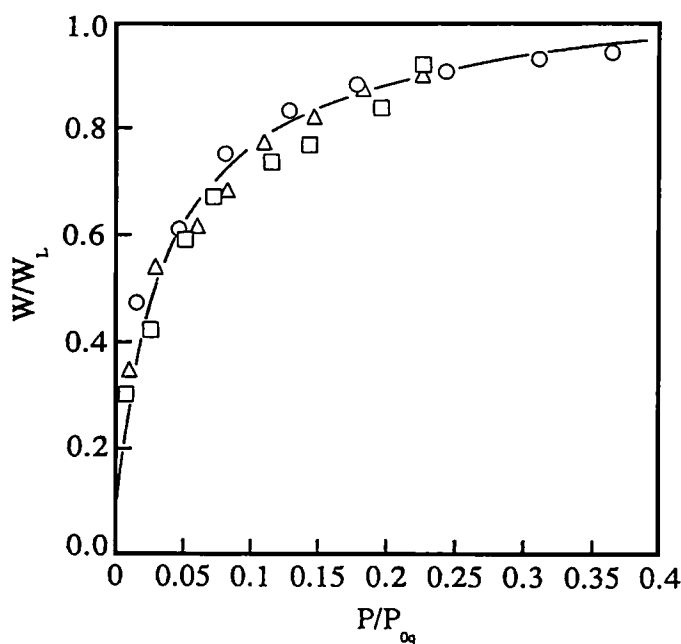


Figure 6. The reduced adsorption isotherm of NO on Fe-ACF. Δ : 274 K, \circ : 303 K, \square : 373 K.

6. Micropore Filling of Supercritical N₂

The separation of supercritical N₂ and O₂ is essentially important in the separation technology. The fundamental adsorption study on supercritical N₂ has been requested. The adsorption isotherms of supercritical N₂ on ACFs were determined at 303 K over the pressure range up to 10 MPa. Five kinds of pitch-based ACFs of different micropore widths were used (micropore width: P5; 0.75 nm, P10; 0.79 nm, P15; 1.01 nm, P20; 1.13 nm, and P25; 1.45 nm). The high pressure adsorption isotherms of N₂ on ACFs at 303 K are shown in Fig. 7. The ordinate in Fig. 7 is expressed by the fractional filling which is the ratio of the amount of high pressure adsorption in mlg^{-1} to the micropore volume W_0 determined by the low pressure N₂ adsorption at 77 K. Here the amount of the supercritical N₂ adsorption was obtained using the liquid density of N₂ (0.808 gml^{-1}). The fractional filling of each ACF depends on the micropore width. The smaller the pore width, the greater the fractional filling. All adsorption isotherms are Langmuirian; the inherent micropore volume W_L was determined by the Langmuir plot. The

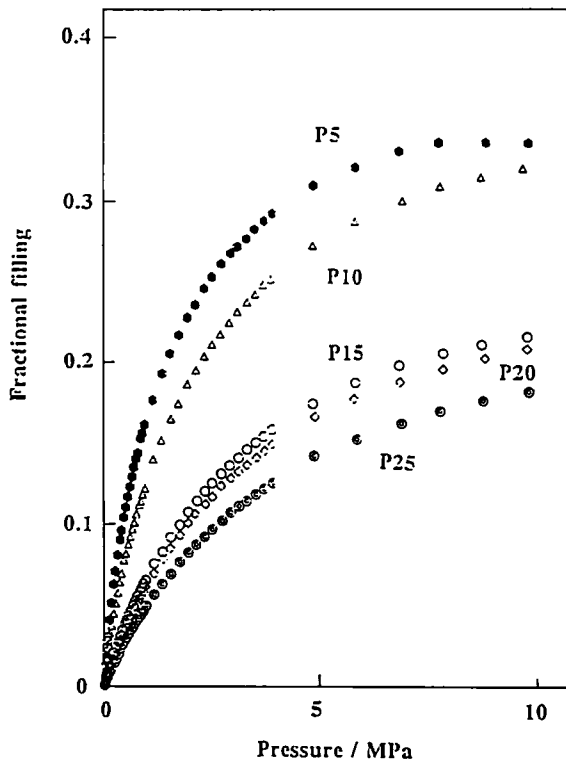


Figure 7. The high pressure adsorption isotherms of N₂ at 303 K.

Table 2. Inherent micropore volume W_L , saturated vapor pressure P_{0q} , and isosteric heat of adsorption $q_{st,\phi=1/e}$ for supercritical N₂ and $q_{st,\phi=1/e}$ (77 K) for vapor N₂ at 77 K on ACF.

	W_L mlg^{-1}	P_{0q} MPa	$q_{st,\phi=1/e}$ kJmol^{-1}	$q_{st,\phi=1/e}$ (77 K) kJmol^{-1}
P5	0.14	23.4	14.2	12.8
P10	0.20	38.6	14.4	11.8
P15	0.23	50.7	14.2	12.3
P20	0.28	57.0	13.8	11.4
P25	0.35	63.6	14.1	10.8

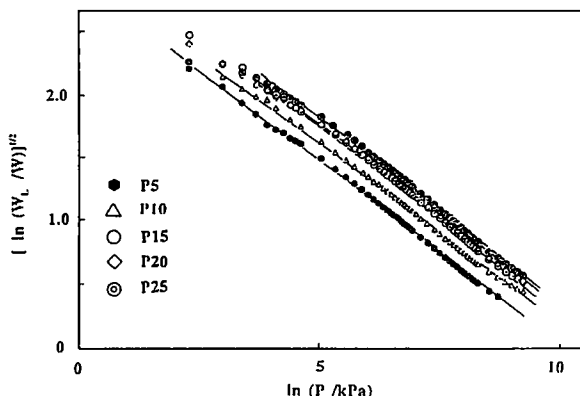


Figure 8. The supercritical DR plots for the high pressure adsorption isotherms of supercritical N₂.

ratio of W_L to W_0 is 0.26 to 0.43; the ratio increases with the decrease of the average micropore width. These adsorption isotherms of supercritical N₂ at 303 K are expressed by linear supercritical DR plots, as shown in Fig. 8. Figure 8 show a good linear relationship over a wide pressure range. The deviation from the linearity at the lower pressure region should come from the very low fractional filling of <0.1%, where the potential theory should be inappropriate. The supercritical DR plot provides the P_{0q} and βE_0 (or $q_{st,\phi=1/e}$). The P_{0q} and $q_{st,\phi=1/e}$ values are collected in Table 2. The P_{0q} for ACF samples is near 50 MPa and depends on the micropore width; the smaller the micropore width, the smaller the P_{0q} . The P_{0q} value is much greater than that of supercritical NO, which is consistent with the difference in the intermolecular interaction; NO molecules form the stabilized dimer, whereas the gas phase dimerization energy of N₂ is only 1.5 kJmol^{-1} (Berns and Avoyd, 1980). Although it is quite difficult to evidence the dimerization of N₂ adsorbed in the micropore, cluster formation of O₂ in the micropore was clearly shown

using the low temperature magnetic susceptibility measurement (Kanoh and Kaneko, 1996). The determined $q_{st,\phi=1/e}$ for supercritical N₂ at 303 K is compared with that for N₂ vapor at 77 K in Table 2. Those values are close to each other. The $q_{st,\phi=1/e}$ of supercritical N₂ is greater than that of vapor N₂ by only 1–3 kJmol⁻¹. Therefore, the adsorbed state of supercritical N₂ is essentially the same as that of the N₂ vapor in the micropore at 77 K. As only micropores having sufficiently great molecular field can be available for inherent micropores for supercritical N₂, $q_{st,\phi=1/e}$ for supercritical N₂ is slightly greater than that for vapor N₂.

The reduced adsorption isotherm for five adsorption isotherms for supercritical N₂ is shown in Fig. 9. The reduced adsorption isotherm is of Type I, being the presence of the micropore filling process. The mutual coincidence of five isotherms is excellent, supporting the powerful applicability of the quasi-vaporization adsorption mechanism even for the high pressure adsorption. This reduced adsorption isotherm was described by the reduced DR equation (Eq. (8)) with $\beta E_0 = 8.8$ kJmol⁻¹, which agrees with that for micropore

filling of N₂ vapor at 77 K (7.5–9.3 kJmol⁻¹). This fact also indicates that high pressure adsorption process of supercritical N₂ is identical to micropore filling of N₂ vapor at 77 K by specific micropores having a sufficiently strong molecular field and supports the goodness of the proposed quasi-vaporization adsorption mechanism.

7. Micropore Filling of Supercritical CH₄

Methane is the main constituent of natural gas. Adsorption of methane at ambient temperature has been studied with a special relevance to methane storage. We used three kinds of HSACs in addition to the pitch-based ACFs (P10 and P20) for high pressure methane adsorption. The HSACs are AX21, aM-24, and Msorb-24. Here AX21 is the high surface area carbon produced by Amoco Co., aM-24 is an activated mesocarbon microbeads (Osaka Gas Co.), and Msorb-24 was supplied by Kansai Coke Co. The microporosity determined by SPE method of N₂ adsorption isotherm at 77 K is shown in Table 3. The surface area of HSACs is greater than 2400 m²g⁻¹, and the pore width is different from each other (Murata and Kaneko).

The adsorption isotherms of supercritical CH₄ were measured gravimetrically up to 10 MPa. Figure 10 shows the CH₄ adsorption isotherms of five activated carbon samples at 303 K. All the adsorption isotherms are Langmuirian, giving the inherent micropore volume W_L for CH₄. As the surface areas of these ACFs are smaller than those of HSACs, the amount of CH₄ adsorption per unit weight of ACF is much smaller than that of HSAC. However, the amount of CH₄ adsorption of ACF is greater in terms of the amount of CH₄ adsorption per the micropore volume due to a stronger micropore field. HSAC samples have a slightly

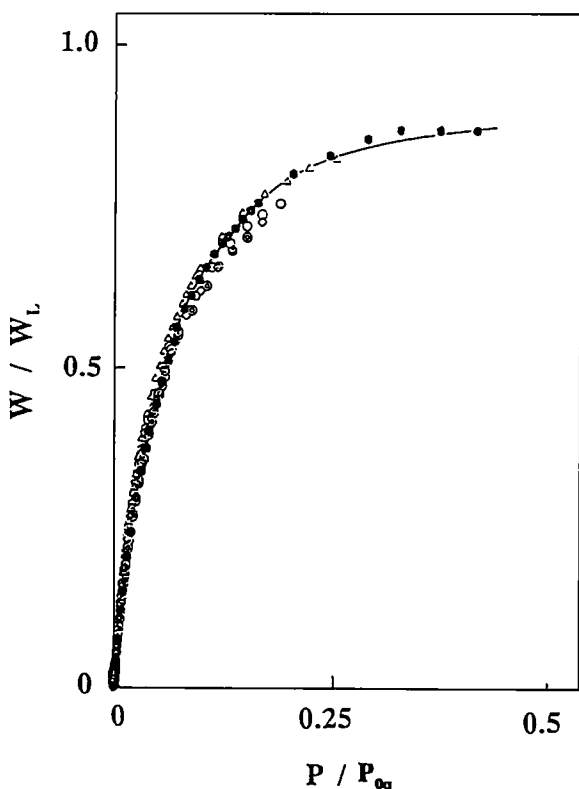


Figure 9. The reduced adsorption isotherms of N₂ at 303 K from five adsorption isotherms.

Table 3. Micropore parameters of activated carbons for adsorption measurement of supercritical CH₄.

Sample	Micropore volume mg ⁻¹	Surface area m ² g ⁻¹	Pore width nm
P10	0.45	1140	0.79
P20	0.97	1765	1.13
AX21	1.49	2400	1.30
MgO-AX21	1.01	1330	1.56
aM-24	1.76	2400	1.60
Msorb-24	1.44	2430	1.22

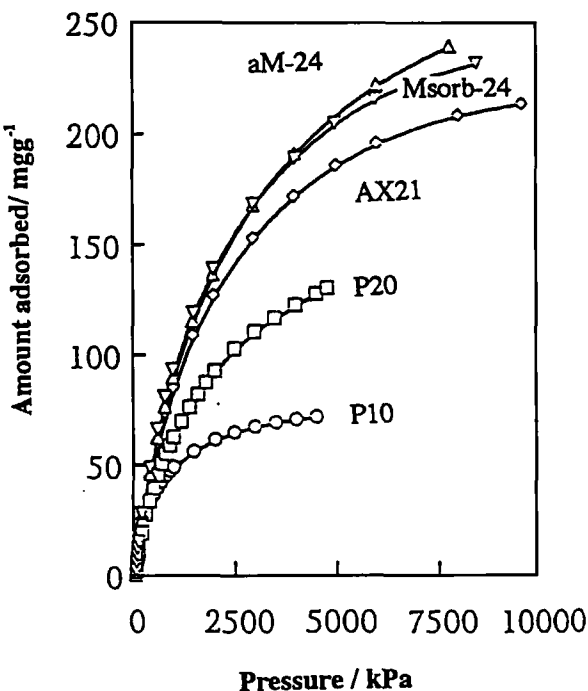


Figure 10. The adsorption isotherms of CH_4 on ACFs and HSACs at 303 K.

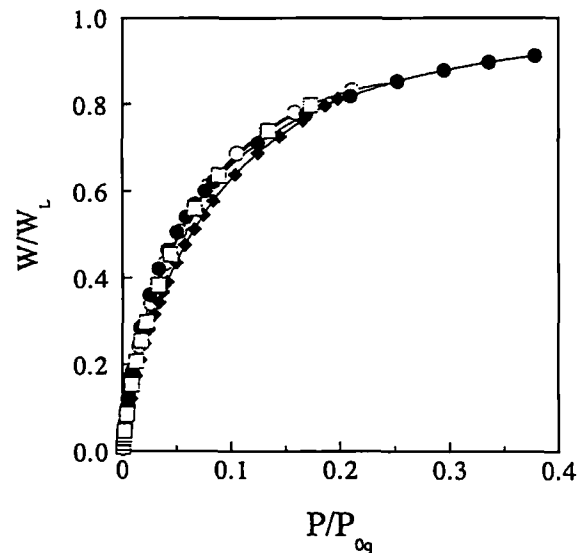


Figure 11. The reduced adsorption isotherms of CH_4 at 303 K. P10: \circ , P20: \bullet , AX21: \blacklozenge , aM-24: \square .

different amount of adsorption each other, which should come from the little difference in the micropore field strength. These adsorption isotherms are well expressed by the supercritical DR equation as well as the adsorption isotherms of supercritical NO_x

and N_2 . The obtained P_{0q} values were in the range of 12–45 MPa and $q_{st,\phi=1/e}$ values were the same each other (17 kJmol^{-1}). Figure 11 shows the reduced adsorption isotherms for supercritical methane. All reduced isotherms are quite close to each other, indicating that the main controlling factor of supercritical CH_4 adsorption is the micropore field strength.

In the above it was shown that adsorption data on three kinds of supercritical gases are described by the supercritical DR equation based on quasi-vaporization adsorption mechanism. As the quasi-vaporization adsorption mechanism should be improved to be more widely applicable, one possible direction of this model will be shown in the following.

8. Organized and Confined Fluids in a Micropore

As all of the quasi-vaporized molecules of supercritical gas in the micropore are not perfectly adsorbed in the micropore, there should be two phases in the micropore. The presence of two phases of a fluid can be evidenced by a thermodynamic approach. The supercritical DR analysis provides the P_{0q} of the quasi-vaporized fluid, and thereby the temperature dependence of P_{0q} should suggest the macroscopic state of the quasi-vaporized fluid.

We examined the high pressure adsorption measurement of CH_4 on AX21 and MgO-AX21 at different temperatures in a similar way described above. MgO-AX21 denotes the fine MgO particles-dispersed AX21; 3–4 wt% $\text{Mg}(\text{OH})_2$ particles are deposited on AX21 and heated at 573 K. The microporosity of MgO-AX21 is also shown in Table 3. Figure 12 shows the temperature dependence of CH_4 adsorption isotherms of AX21 and MgO-AX21. The dispersion of MgO enhances the CH_4 adsorption noticeably. The marked enhancement effect of MgO dispersion on CH_4 adsorption was observed in case of ACF in the preceding letter (Kaneko et al., 1993). Although the exact mechanism on the enhancement effect is not clear, a weak chemisorptive interaction of the dispersed MgO with supercritical CH_4 should be associated with it. The lower the adsorption temperature, the greater the amount of CH_4 adsorption. This adsorption behavior is indicative of a typical physical adsorption in Fig. 12.

The supercritical DR analysis was applied to these adsorption isotherms, leading to the P_{0q} as a function of adsorption temperature. Figure 13 shows the van't Hoff plots of P_{0q} for AX21 and MgO-AX21. The good linearity evidences the presence of the thermodynamic

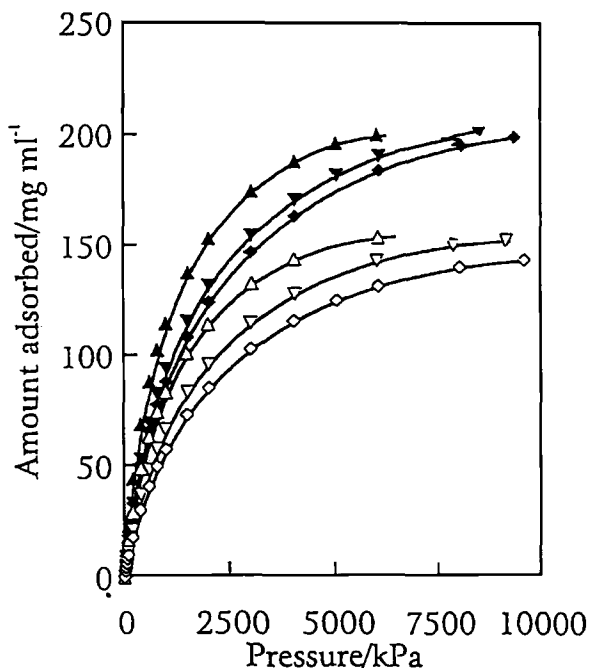


Figure 12. The temperature dependence of the adsorption isotherms of CH_4 on AX21 and MgO-AX21. AX21 Δ : 273K, ∇ : 297 K, \diamond : 303 K; MgO-AX21 \blacktriangle : 273K, \blacktriangledown : 297K, \blacklozenge : 303K.

equilibrium between two phases. The slope of the van't Hoff plot provides the enthalpy change, ΔH_t , between two phases. Table 4 shows ΔH_t values for AX21 and MgO-AX21 and the ΔH_v of bulk CH_4 is shown for comparison. The ΔH_t for MgO-AX21 is greater than that for AX21, which indicates the stabilization of the adsorbed state of CH_4 in the micropore of MgO-AX21. The ΔH_t values are much greater than ΔH_v of bulk CH_4 . This difference suggests that the adsorbed state of CH_4 is more stabilized than the bulk liquid state of CH_4 . Therefore we must distinguish the adsorbed phase in the micropore from the bulk liquid phase. We propose to designate organized and confined fluid fluids for two phases. The organized fluid corresponds to the adsorbed molecular aggregate thorough quasi-vaporization, whereas the confined fluid is used for the quasi-vapor in the micropore. As the molecular density of the confined fluid is much less than that of the organized fluid, the amount of the adsorption is mainly determined by the amount of the organized fluid. The ΔH_t is the enthalpy change of the transition from the organized fluid to confined fluid.

The further discussion on this model will be given in future. This model should be helpful to understand the state of fluids in small pore system.

Table 4. Enthalpy change ΔH_t for transition of organized fluid to confined fluid for supercritical CH_4 on AX21 and MgO-AX21.

	$\Delta H_t \text{ kJ mol}^{-1}$
AX21	13.2
MgO-AX21	16.0
Enthalpy change of vaporization for bulk CH_4	8.18

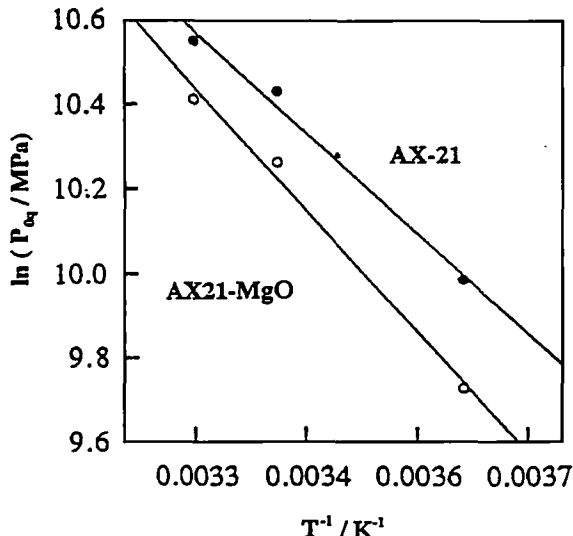


Figure 13. The van't Hoff plots of the p_{0q} of CH_4 for AX21 and MgO-AX21.

Acknowledgments

The authors would like to aknowledge the Grant-in-Aids from the Ministry of Education and Science, Japanese Government and the finacial support from the Japan Gas Association.

References

- Adamson, A.W., *Physical Chemistry of Surfaces*, John Wiley & Sons, Chap. 16, 1990.
- Atkins, P.W., *Physical Chemistry*, Oxford University Press, Chap. 1, 1990.
- Balbuena, P.B. and K.E. Gubbins, "Classification of Adsorption Behavior: Simple Fluids in Pores of Slit-Shaped Geometry," *Fluid Phase Equilibria*, **76**, 21 (1992).
- Bering, B.P., M.M. Dubinin, and V.V. Serpinsky, "Theory of Volume Filling for Vapor Adsorption," *J. Colloid Interface Sci.*, **21**, 378 (1966).

Berns, R.M. and A.V. Avoird, "N₂-N₂ Interaction Potential from ab Initio Calculations, with Application to the Structure of (N₂)₂," *J. Chem. Phys.*, **72**, 6107 (1980).

Bojan, B.P., E. Cheng, M.W. Cole, and W.A. Steele, "Topologies of Capillary Condensation," *Adsorption*, **2**, 57 (1996).

Cheng, S.G. and R.T. Yang, "Theoretical Basis for the Potential Theory Adsorption Isotherms. The Dubinin-Radushkevich and Dubinin-Astakov Equations," *Langmuir*, **10**, 4244 (1994).

Cracknell, R.F., K.E. Gubbins, M. Maddox, and D. Nicholson, "Modeling Fluid Behavior in Well-Characterized Porous Materials," *Account Chem. Res.*, **28**, 281 (1995).

Drago, S.R., D.S. Burns, and T.J. Lafrenz, "A New Adsorption Model for Analyzing Gas-Solid Equilibria in Porous Materials," *J. Phys. Chem.*, **100**, 1718 (1996).

Dubinin, M.M., "The Potential Theory of Adsorption of Gases and Vapors for Adsorbents with Energetically Nonuniform Surfaces," *Chem. Rev.*, **60**, 235 (1960).

Dubinin, M.M., "Adsorption Properties and Microporous Structures of Carbonous Adsorbents," *Carbon*, **25**, 593 (1987).

Dunne, J.A., A.L. Myers, and D.A. Kofke, "Simulation of Adsorption of Liquid Mixtures of N₂ and O₂ in a Model Faujasite Cavity at 77.5 K," *Adsorption*, **2**, 41 (1996).

Everett, D.H. and J.C. Powl, "Adsorption in Slit-Like and Cylindrical Micropores in the Henry's Law Region," *J. Chem. Soc. Faraday Trans. 1*, **72**, 619 (1976).

Fujie, K., S. Minagawa, T. Suzuki, and K. Kaneko, "NO/H₂O Clathrate Formation in Subnano Graphitic Slit Space," *Chem. Phys. Lett.*, **236**, 427 (1995).

Gregg, S.J. and K.S.W. Sing, *Adsorption, Surface Area, and Porosity*, Academic Press, 1982.

Hill, T.L., "Theory of Physical Adsorption," *Adv. Catal.*, **4**, 211 (1952).

Horvath, G. and K. Kawazoe, "Method for the Calculation of Effective Pore Size Distribution in Molecular Sieve Carbon," *J. Chem. Eng., Japan*, **16**, 470 (1983).

Iiyama, T., K. Nishikawa, T. Otowa, and K. Kaneko, "An Ordered Water Molecular Structure in a Slit-Shaped Carbon Nanospace," *J. Phys. Chem.*, **99**, 10075 (1995).

Jagiello, J., T.J. Bandosz, K. Putyera, and J.A. Schwarz, "Adsorption Near Ambient Temperatures of Methane, Carbon Tetrafluoride, and Sulfur Hexafluoride on Commercial Activated Carbons," *J. Chem. Eng. Data*, **40**, 1288 (1995).

Jaroniec, M. and R. Maday, "Physical Adsorption on Heterogeneous Solids," Elsevier, 1988.

Kakei, K., S. Ozeki, T. Suzuki, and K. Kaneko, "Multistage Micropore Filling Mechanism of Nitrogen on Microporous and Micrographitic Carbons," *J. Chem. Soc. Faraday Trans.*, **86**, 371 (1991).

Kaneko, K., "Anomalous Micropore Filling of NO on α -FeOOH-Dispersed Activated Carbon Fibers," *Langmuir*, **3**, 357 (1987).

Kaneko, K., "Anomalous Micropore Filling of NO on Fe₂O₃-Dispersed Activated Carbon Fibers, Characterization of Porous Solids I," Elsevier, p. 183, 1988.

Kaneko, K., "Effect of Temperature on Micropore Filling of Supercritical NO on Fe₂O₃-Dispersed Activated Carbon Fibers," *Colloid Surfaces*, **37**, 115 (1989).

Kaneko, K., "Molecular Assembly Formation in a Solid Nanospace," *Colloid Surface*, **109**, 319 (1996).

Kaneko, K., R. Cracknell, and D. Nicholson, "Nitrogen Adsorption in Slit Pores at Ambient Temperatures: Comparison of Simulation and Experiment," *Langmuir*, **10**, 4606 (1994).

Kaneko, K., N. Fukuzaki, K. Kakei, T. Suzuki, and S. Ozeki, "Enhancement of NO Dimerization by Micropore Fields of Activated Carbon Fibers," *Langmuir*, **5**, 960 (1989).

Kaneko, K. and C. Ishii, "Superhigh Surface Area-Determination of Microporous Solids," *Colloid Surf.*, **67**, 203 (1992).

Kaneko, K., C. Ishii, M. Ruike, and M. Kuwabara, "Origin of Superhigh Surface Area and Microcrystalline Graphitic Structures of Activated Carbons," *Carbon*, **30**, 1075 (1992).

Kaneko, K., A. Kobayashi, T. Suzuki, S. Ozeki, K. Kakei, N. Kosugi, and H. Kuroda, "The Dimer State of NO in Micropores of Cu(OH)₂ Dispersed Activated Carbon Fibers," *J. Chem. Soc. Faraday Trans. 1*, **84**, 1795 (1988).

Kaneko, K., K. Shimizu, and T. Suzuki, "Intrapore Field-Dependent Micropore Filling of Supercritical N₂ in Slit-Shaped Micropores," *J. Chem. Phys.*, **97**, 8705 (1992).

Kanoh, H. and K. Kaneko, "Magnetic Spin States of O₂ Confined in a Graphitic Slit-Shaped Nanospace at Low Temperature," *J. Phys. Chem.*, **100**, 755 (1996).

Murata, K. and K. Kaneko, "Basic Oxide-Dispersion Induced Enhancement of Micropore Filling of Methane," *J. Chem. Soc. Faraday Trans.*, to be submitted.

Rao, A.M., A.W.P. Fung, M.S. Dresselhaus, and M. Endo, "Structural Characterization of Heat-Treated Activated Carbon Fibers," *J. Mater. CVRes.*, **7**, 1788 (1992).

Rudzinski, W. and D.H. Everett, "Adsorption of Gases on Heterogeneous Surfaces," Academic Press, 1992.

Setoyama, N., M. Ruike, T. Kasu, T. Suzuki, and K. Kaneko, "Surface Characterization of Microporous Solids With He Adsorption and Small Angle X-Ray Scattering," *Langmuir*, **9**, 2612 (1993).

Sing, K.S.W., "The Use of Physisorption for the Characterization of Microporous Carbons," *Carbon*, **27**, 5 (1989).

Steele, W.A., "The Physical Interaction of Gases with Crystalline Solids," *Surface Sci.*, **36**, 317 (1973).

Wakasugi, Y., S. Ozawa, and Y. Ogino, "Physical Adsorption of Gases at High Pressure," *J. Colloid Interface Sci.*, **79**, 399 (1981).

Wang, Z.M., T. Suzuki, N. Uekawa, K. Asakura, and K. Kaneko, "Mixed Valence Oxide-Dispersion Induced Micropore Filling of Supercritical NO," *J. Phys. Chem.*, **96**, 10917 (1992).